Available online at www.sciencedirect.com
SCIENCE DIRECT®
Solar Energy Materials & Solar Cells
ELSEVIER
Solar Energy Materials & Solar Cells 82 (2004) 291–298
www.elsevier.com/locate/solmat

$Au–Al_2O_3$ nanocomposites: XPS and FTIR spectroscopic studies

J. García-Serrano[a,b], A.G. Galindo[c], U. Pal[a,*]

[a] *Instituto de Física, Universidad Autónoma de Puebla, Apdo. Postal J-48, Puebla, Pue., C.P. 72570, Mexico*
[b] *Centro de Investigaciones en Materiales y Metalurgia, Universidad Autónoma del Estado de Hidalgo, Carretera Pachuca Tulancingo Km 4.5, C. P. 42184, Pachuca, Hgo., Mexico*
[c] *Centro de Química, Instituto de Ciencias, Benemérita Universidad Autónoma de Puebla, Blvd. 14 sur 6301, San Manuel 72570, Puebla, Pue., Mexico*

Abstract

$Au–Al_2O_3$ nanocomposite films are prepared with different Au contents on quartz substrates by radio frequency co-sputtering technique and annealed at different temperatures. The interactions between the Au nanoparticles and alumina matrix have been studied using X-ray photoelectron spectroscopy (XPS) and infrared spectroscopy (IR). XPS analysis reveals that both the Al and O atoms of the matrix are affected by the presence of Au nanoparticles and also by annealing the samples. For the as-grown example, the Al 2p peak shifts towards higher energy upon metal incorporation, whereas O 1s peak shifts towards lower binding energy. The shift of the binding energies could be due to the redistribution of electronic charge in Al_2O_3 caused by the incorporation of the Au nanoparticles. Due to the high electronegativity, the incorporated Au does not form any oxide in alumina. On the other hand, Al of the alumina matrix forms Al_2Au alloy at the metal–oxide interface at room temperature. Annealing the composites at temperatures higher than 200°C breaks the Al_2Au alloy leaving the Au in its elemental state. Infrared absorption measurements reveal the formation of Au_3 clusters in alumina due to Au incorporation. Evolutions of the metal–oxide interface state and IR absorption peak with the variation of annealing temperature of the films has been studied.

Keywords: Nanocomposites; Gold; X-ray photoelectron spectroscopy; Infrared absorption spectroscopy

*Corresponding author. Tel.: +52-222-2295500; fax: +52-222-2295611.
E-mail address: upal@sirio.ifuap.buap.mx (U. Pal).

0927-0248/$ - see front matter © 2004 Elsevier B.V. All rights reserved.
doi:10.1016/j.solmat.2004.01.026

1. Introduction

Most of the properties of metal–oxide materials are governed from the interface phenomena like the formation of new compounds, electron transfer and electrostatic interaction. Surface analysis methods like Auger electron spectroscopy (AES) and X-ray photoelectron spectroscopy (XPS) are the useful techniques for the study of metal–oxide interactions like electronic structure of the substrate and electronegativity of the deposited metal [1,2] along with the estimation of charge variation of metal atoms in oxide atmosphere [3,4]. Several works have been published on the determination of Auger parameters to study the above-mentioned effects in metal–oxide composite systems [5–8]. However, most of them deal with the metal deposited surfaces of oxide substrates. For example, evolution of metal–oxide interface has been studied by Ealet and Gillet [8] for metals of different electronegativities on alumina surface by AES technique. The electronegativity of the deposited metals determines the possibility of formation of their oxides or new compounds when they are incorporated in an oxide environment.

Where the study of metal–oxide interface on metal deposited oxide substrates is very important for acquiring the basic knowledge on the mechanism of interaction, a similar study/evaluation in a bulk metal–oxide composite is very important for its technological applications.

There has been a great interest on the growth and characterization of metal nano-cluster composites in recent years due to their large non-linear optical susceptibility [9–11], potential applications in chemical catalysis, electronics and photonic materials [12–15]. In case of metal–oxide composites, SiO_2 is the mostly used host material. On the other hand, incorporation of metal clusters in functional matrices like ZnO, TiO_2, MgO and Al_2O_3 is relatively recent [16–20]. Incorporation of metal clusters in such functional matrices has some special advantage for their applications in catalysis and electrolysis. However, for their applications, the study of metal–oxide interface is very important.

In the present work we present the evolution of metal–oxide interface in the Au–Al_2O_3 nanocomposite films prepared by r.f. co-sputtering technique. Effect of annealing temperature on the chemical state of Au in the alumina matrix environment has been studied by XPS technique. Fourier Transform Infrared (FTIR) absorption technique has been used to study the chemical and vibrational states of the Au atoms beyond the interface. It has been observed that due to the high electronegativity of Au, it does not form any oxide on incorporation in alumina matrix; whereas it forms an alloy with the Al of the alumina matrix. Annealing the composite films at temperatures above 200°C causes the dissociation of the latter alloy due to the reduction of the solubility of Au in alumina matrix. Beyond the interface, the incorporated Au in the alumina matrix remains in its trimmer Au_3 cluster form.

2. Experimental

Au–Al_2O_3 composite films were prepared on quartz glass substrates by co-sputtering of Au and Al_2O_3 using an r.f. sputtering apparatus. Three pieces of Au wires (0.5 mm diameter, 99.999% Purity) of different lengths (1, 3, and 6 mm) were placed symmetrically on a 50 mm diameter Al_2O_3 target (99.99% Purity) and sputtered with 150 W r.f. power at 15 mTorr Ar gas pressure. The content of Au in the samples was varied by varying the length of Au wires on the Al_2O_3 target. The as-deposited films were annealed at 200°C, 400°C and 600°C for 2 h in argon atmosphere. For the TEM observations, the composite films were deposited on carbon-coated NaCl substrates and transferred subsequently to the copper grids. The microstructure of the composite was observed by a JOEL-2010 transmission electron microscope. The composition and chemical states of the elements in the films were studied by a Perkin-Elmer (PHI 5600ci) XPS system. For XPS measurements the AlK_α line (1486.6 eV) was used. A Nicollet Magna 750 FTIR spectrometer was used to record the diffuse reflectance spectra of the composite films.

3. Results and discussion

3.1. Transmission electron microscopy

Fig. 1 shows the typical TEM microphotographs of as-deposited Au–Al_2O_3 composite films prepared with different Au contents. Formation of Au nanoparticles in the films is evident, which are dispersed uniformly in the matrix. In the films prepared with three pieces of Au wires of 1 mm length, the average size of the Au particles was 3.2 nm. The increment of Au content in the composite

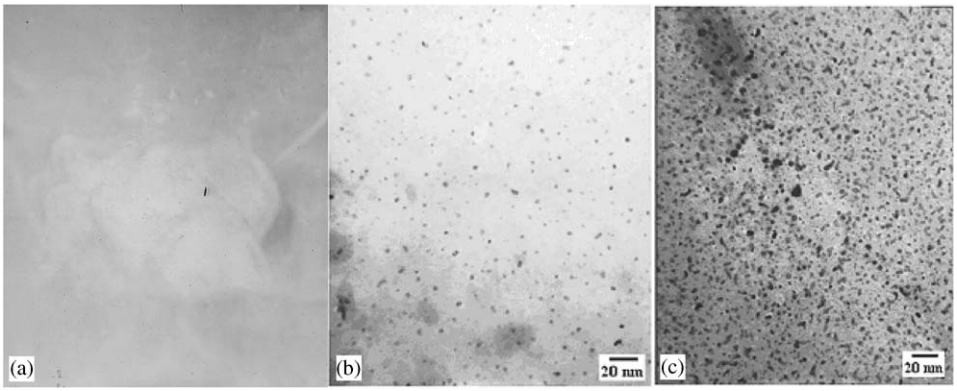

Fig. 1. Typical TEM micrographs of: (a) the matrix Al_2O_3 and of as-deposited Au–Al_2O_3 composite thin films prepared with three pieces of Au wires of: (b) 1 mm; and (c) 3 mm length.

films caused a small increment in the average size of the particles. For the films prepared with Au wires of 3 mm length, the average size of the nanoparticles was 5.1 nm.

Fig. 2 presents the typical micrographs of Au–Al_2O_3 composite films annealed at different temperatures. When the films were annealed at 200°C, the dimension of the particles did not increase noticeably. However, when the annealing temperature of the samples increased to 400°C and 600°C, the small Au particles aggregated to form bigger particles, with an average size of 25 and 46 nm, respectively. In general, the average particle size depends on the annealing temperature. The results suggest that the size of the Au particles in the Al_2O_3 matrix can be controlled by adjusting the annealing temperature.

3.2. X-ray photoelectron spectroscopy

The metal–matrix interaction in the Au–Al_2O_3 nanocomposite films was studied using XPS. Fig. 3 shows the core level XPS spectra in the Al 2p, Au 4f and O 1s regions for Au–Al_2O_3 nanocomposites annealed at different temperatures. We can observe that the peak with a binding energy of ~74 eV (associated to Al 2p emission) shifts towards higher energy with the increase of annealing temperature. Whereas, the O 1s peak (located at about 531 eV) shifts towards lower binding energy. The position of XPS Au 4f peaks depends strongly on the chemical/electronic environment surrounding it. The peaks located at around 83.5 and 87 eV were assigned to the spin–orbit splitted components of the Au-4f level in the pure Au metal [21]. Whereas, the remaining peaks (above 90.0 eV) represent the emissions from the Au-4f within a different chemical environment. It is well established that the binding energy shifts are characteristic of physical or chemical change in the environment of the analyzed species. On the other hand, it has been observed that the electronegativity of the incorporated metal plays a decisive role on the type of interaction between the metal and alumina [8]. When the incorporated atoms have a

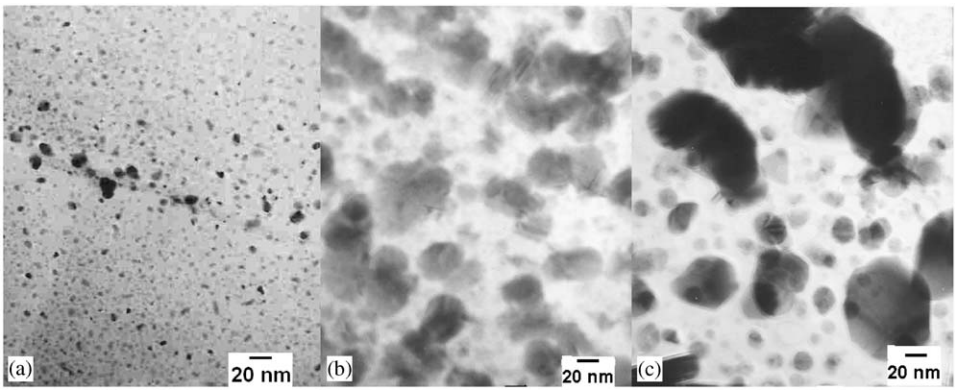

Fig. 2. Typical TEM micrographs of Au–Al_2O_3 composite films prepared with 3 pieces of Au wires of 3 mm length and annealed at: (a) 200°C; (b) 400°C; and (c) 600°C.

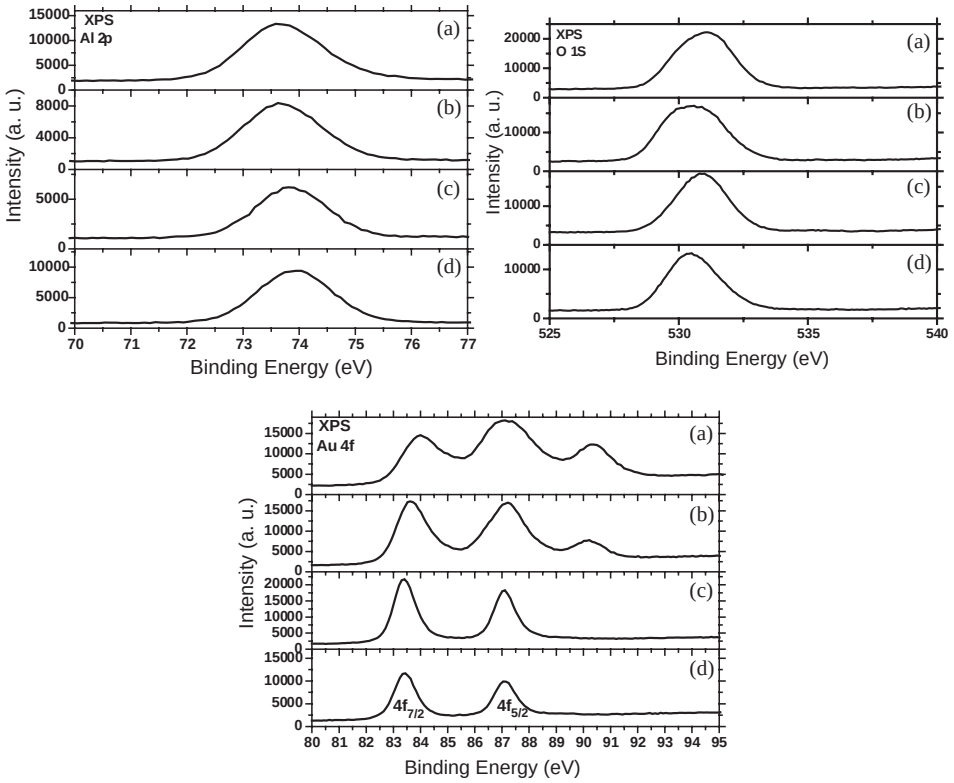

Fig. 3. X-ray photoelectron spectra of Au–Al_2O_3 composite films prepared with three pieces of Au wires of 3 mm length: (a) as-grown; (b), (c) and (d) annealed at 200°C, 400°C and 600°C, respectively. The figure shows the chemical shift in the Al 2p, O 1s and Au 4f regions.

higher electronegativity, the interaction is characterized by an electron transfer from the oxide to the metal [8]. In our case, as the electronegativity of Au (2.2 in the Pauling scale) is very high, a transfer of electrons from oxide (Al_2O_3) to the metal is possible. From Fig. 3C, we can observe that the Au $4f_{5/2}$ peak position shifted to lower energy with respect to that of pure gold (88.0 eV) for the annealed samples. As the transfer of electrons from the matrix to gold particles is equivalent to the reduction process of gold, the lower energy shift of the Au 4f band is expected. Due to the same reason, the formation of gold oxide is less probable. It is to be noted that in none of the samples we could detect the formation of gold oxide. However for the untreated sample and 200°C annealed samples, there appeared a peak at about 90.40 and 90.20 eV, respectively. The peak positions did not suggest the formation of any oxide species of gold. We assigned the peak as the Au $4f_{5/2}$ emission band of Al_2Au alloy formed in the as-grown composites. The position of the peak shifted a bit towards higher energy in comparison with the reported value (89.5 eV) by Piao and McIntyre [22] in thin film gold–aluminum alloy, due to the partial oxidation of the alloy. On annealing the samples at 200°C, the alloy oxide reduces, causing a shift of

the peak position towards lower energy (90.20 eV). However, on annealing the samples at higher temperatures, apart from the reduction of the alloy oxide, due to the reduction of solubility of Au in alumina, the alloy dissociates to form pure gold. The formation of bigger aggregates of Au in the samples annealed at temperatures above 200°C supports the above argument.

3.3. Infrared spectroscopy

IR absorption of the Au–Al_2O_3 nanocomposite films have been studied for the 100–2500 cm^{-1} spectral range. For the spectral range 400–2500 cm^{-1} there appeared only the absorption bands corresponding to the quartz substrates except a small peak at about 530 cm^{-1} related to the alumina matrix (Fig. 4). There appeared no absorption band related to the oxide state of gold for any sample. In Fig. 5, the IR absorption spectra of the composite films for the 100–400 cm^{-1} spectral range are presented. For all the composite films, the IR spectra revealed only one absorption peak located at around 151 cm^{-1}, intensity of which increases gradually depending on their Au content and annealing temperature. This absorption peak is tentatively assigned to the stretching symmetric (SS) vibrational mode of gold trimer (Au_3). The position of our experimental peak is very close to the calculated vibrational frequency [23] for Au_3 clusters. With the increase of the annealing temperature, there was no significant change in the peak position.

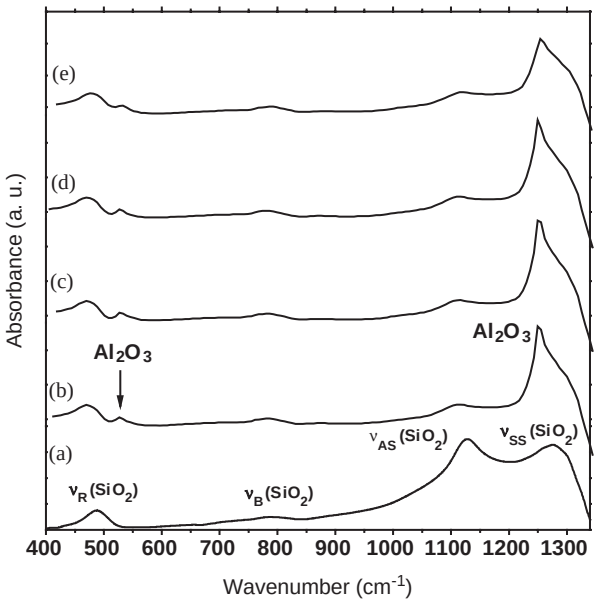

Fig. 4. FTIR diffuse reflectance spectra in the region of 400–1340 cm^{-1} of: (a) quartz; (b) Al_2O_3 matrix; and (c); (d); (e) as-grown Au–Al_2O_3 nanocomposite films prepared with Au wires of 1, 3 and 6 mm length, respectively.

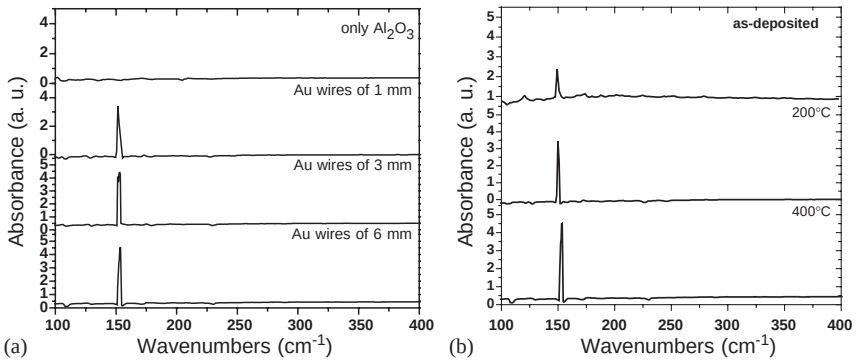

Fig. 5. FT–IR diffuse reflectance spectra in the region of 100–400 cm^{-1} of Au–Al_2O_3 nanocomposite films: (a) prepared with different Au content and annealed at 400°C; (b) prepared with Au wires of 6 mm and annealed at different temperatures.

4. Conclusions

The incorporation of Au in alumina matrix by sputtering produces Au nanoparticles, the size of which depends mainly on the temperature of annealing due to the strong temperature dependence of Au solubility in alumina. Due to the high the electronegativity of Au, the incorporated Au remains in elemental state without forming any oxide species. However, a part of incorporated Au in alumina forms the Al_2Au alloy at the metal–alumina interface at room temperature. On annealing the samples at temperatures higher than 200°C, the alloy dissociates. The incorporated Au remains in the Au_3 cluster form inside the metal particles. On increasing the annealing temperature, due to the breaking of Al_2Au alloy and hence availability of more elemental Au in the composites, the intensity of the Au_3 IR absorption band increases.

Acknowledgements

U. Pal acknowledges the partial financial support of VIEP-CONCyT-SEP, Mexico through the grant No. II013I02.

References

[1] E. Gillet, B. Ealet, Surf. Sci. 273 (1992) 427.
[2] B. Ealet, Thesis, Université Aix-Marseille III, 1993.
[3] C.D. Wagner, H.A. Six, W.T. Jansen, J.A. Taylor, Appl. Surf. Sci. 9 (1981) 203.
[4] C.D. Wagner, A. Joshi, J. Electron. Spectrosc. Relat. Phenom. 47 (1988) 283.
[5] G. Moretti, P. Porta, Surf. Interface 16 (1990) 159.
[6] B. Ealet, B. Robrieux, E. Gillet, J. Adhesion Sci. Technol. 6 (1992) 1221.
[7] B. Ealte, E. Gillet, Surf. Sci. 281 (1993) 91.

[8] B. Ealet, E. Gillet, Surf. Sci. 367 (1996) 221.
[9] F. Hache, D. Ricard, C. Flytzanis, U. Kreibig, Appl. Phys. A 47 (1988) 347.
[10] R.F. Haglung Jr., R.H. Magruder III, S.H. Morgan, D.O. Henderson, R.A. Weller, L. Yang, R.A. Zuhr, Nucl. Instrum. Methods B 65 (1992) 405.
[11] R. Bertoncello, F. Trivillin, E. Cattaruzza, P. Mazzoldi, G.W. Arnold, G. Battaglin, M. Catalano, J. Appl. Phys. 77 (1995) 1294.
[12] G.D. Stucky, Nav. Res. Rev. 43 (1991) 28.
[13] J.H. Sinfelt, G.D. Meitzner, Acc. Chem. Res. 26 (1993) 1.
[14] M.L. Steigerwald, L.E. Brus, Acc. Chem. Res. 23 (1990) 183.
[15] H. Weller, Adv. Mater. 5 (1993) 88.
[16] O. Vázquez-Cuchillo, U. Pal, C. Vázquez-López, Solar Energy Mater. Solar Cells 70 (2001) 369.
[17] N. Koshizaki, K. Yasumoto, S. Terauchi, H. Umehara, T. Sasaki, T. Oyama, Nanostruct. Mater. 9 (1997) 147.
[18] T. Sasaki, S. Rozbichi, Y. Matsumoto, N. Koshizaki, S. Koshizaki, H. Umehara, Mater. Res. Soc. Symp. Proc. 457 (1997) 425.
[19] U. Pal, E. Aguila Almanza, O. Vázquez-Cuchillo, N. Koshizaki, T. Sasaki, S. Terauchi, Solar Energy Mater. Solar Cells 70 (2001) 363.
[20] J. García-Serrano, U. Pal, Int. J. Hydrogen Energy 28 (2003) 637.
[21] B. Koslowski, H.G. Boyen, C. Wilderotter, G. Kastle, P. Ziemann, R. Wahrenberg, P. Oelhafen, Surf. Sci. 475 (2001) 1.
[22] H. Piao, N.S. McIntyre, Surf. Sci. 421 (1999) L171.
[23] G. Bravo-Pérez, I.L. Garzón, O. Novaro, Chem. Phys. Lett. 313 (1999) 655.